JOURNAL OF AGRICULTURAL AND FOOD CHEMISTRY
ARTICLE

J. Agric. Food Chem. 2010, 58, 11593–11599 11593
DOI:10.1021/jf101283f

Structural Characterization and Hypoglycemic Effects of Arabinogalactan-Protein from the Tuberous Cortex of the White-Skinned Sweet Potato (*Ipomoea batatas* L.)

Sei Ozaki,*,†,‡ Naoko Oki,† Shiho Suzuki,‡ and Shinichi Kitamura*,‡

†Research Institute, Fuji-Sangyo Company, Ltd., Marugame, Kagawa 763-0071, Japan, and
‡Graduate School of Life and Environmental Sciences, Osaka Prefecture University, Sakai, Osaka 599-8531, Japan

An arabinogalactan-protein (WSSP-AGP) was isolated from the tuberous cortex of the white-skinned sweet potato (WSSP; *Ipomoea batatas* L.). It consists of 95% (w/w) carbohydrate and 5% (w/w) protein with high contents of hydroxyproline, alanine, and serine. Its sugar composition is α-L-Rha:α-L-Ara:β-D-Gal:β-D-GlcA in a molar ratio of 1.0:4.1:7.6:1.3. Its weight-average molecular weight was estimated to be 126800 g/mol by high-performance size exclusion chromatography coupled with multiangle laser light scattering. Structural analysis indicated that WSSP-AGP is a (1→3)-β-D-galactan highly branched at O-6 with (1→6)-β-D-galactan, in which the branched chains are substituted at the O-3 position with α-L-Ara*f*-(1→ and α-L-Ara*f*-(1→5)-α-L-Ara*f*-(1→ and at the O-6 position typically with α-L-Rha*p*-(1→4)-β-D-GlcA*p*-(1→ as terminating groups. Continuous administration of WSSP-AGP to KKA^y mice significantly lowered fasting plasma glucose levels. This indicates that WSSP-AGP plays an important role in the hypoglycemic effects of WSSP.

KEYWORDS: Arabinogalactan-protein; *Ipomoea batatas* L.; acid hydrolysis; NMR; hypoglycemic effects

INTRODUCTION

The white-skinned sweet potato (WSSP) is a kind of sweet potato (*Ipomoea batatas* L.), belonging to the Convolvulaceae family, used as a food and traditional medicine in Minas Gerais, Brazil (*1*), and cultivated and used as a food in Japan. The tuberous root is effective for the improvement of hypertension, hemorrhage, and diabetes mellitus (*2*). We have been studying its antihyperglycemic effects. Some studies involving continuous ingestion of WSSP in various diabetic model animals such as db/db mice, KKA^y mice, and Zucker fa/fa rats have shown that it is effective against hyperglycemia and improves insulin sensitivity (*3*, *4*). Another study on the mode of action in KKA^y mice reported significant enhancement of ACRP30 expression and a tendency to lower TNF-α expression in adipose tissue (*5*). These results suggest that the improvement in secretion of these adipocytokines implicated in insulin resistance in adipose tissue is due to the hypoglycemic effect of WSSP. A similar effect has been confirmed in humans with type 2 diabetes mellitus by Ludvik et al. (*6*−*8*).

WSSP contains some resin glycosides (*1*), but their correlation with antidiabetic effects is unclear. Oke et al. (*9*) found that a 60% ethanol extract of WSSP is effective against hyperglycemia in alloxan-induced diabetic mice, without identifying the active component. Kusano et al. (*10*) were unable to identify the main antidiabetic component, but confirmed that it was present in the tuberous cortex of WSSP. They suggested that it was composed of an acidic glycoprotein with high molecular weight. Plant cell walls are sources of pharmacologically active polysaccharides such as arabinogalactan (*11*), arabinoxylan (*12*), and glucomannan (*13*), which are used to treat cancer, improve the gastrointestinal tract, and lower blood glucose and lipid levels (*11*−*13*). This strongly suggests that the high molecular weight constituents described above may contribute to the physiological effects of WSSP.

In this study we performed isolation and structural analysis to identify the principal antidiabetic constituent of WSSP and evaluated its effects on fasting plasma glucose (FPG) by continuous ingestion in spontaneously diabetic animals.

MATERIALS AND METHODS

Plant Material. *I. batatas* L. was purchased from the Kagawa Prefectural Asa Agricultural Cooperative. We peeled it to obtain the cortex and freeze-dried it.

Isolation of AGP from WSSP (*I. batatas* L.). The dried cortex powder of WSSP (WSSP-cortex, 1 kg) was extracted by stirring in water (10 L) at room temperature for 4 h. The mixture was centrifuged at 12000*g* for 30 min and filtered to obtain the aqueous solution. It was concentrated in vacuo and was dialyzed (MW cutoff 14 kDa, Wako Pure Chemical Industries, Ltd., Osaka, Japan) against deionized water at 4 °C for 3 days to remove low molecular weight constituents. The nondialyzable parts containing soluble and insoluble parts were concentrated in vacuo to prepare a suspension. The suspension was precipitated by the addition of solid ammonium sulfate to reach 1.5 M concentration, followed by centrifugation at 12000*g* for 30 min. The resulting supernatant was loaded onto a hydrophobic interaction chromatographic column of Toyopearl

*Authors to whom correspondence should be addressed [(S.O.) phone +81 877 25 3221, fax +81 877 25 0567, e-mail s_ozaki@fuji-sangyo.co.jp; (S.K.) phone +81 72 254 9866, fax +81 72 254 9937, e-mail skita@bioinfo.osakafu-u.ac.jp].

Published on Web 10/29/2010

Butyl-650 M (240 × 40 mm i.d.; Tosoh Co., Tokyo, Japan), and a crude polysaccharide fraction was collected by elution with 1.5 M ammonium sulfate (500 mL). After dialysis against deionized water at 4 °C for 3 days to desalt, the internal effluent was applied to an anion-exchange column of Toyopearl SuperQ-650 M (200 × 22 mm i.d., Tosoh Co.) as follows: elution with 0.01 M sodium phosphate buffer (pH 7.5) for 90 min, 0−0.15 M NaCl in 0.01 M sodium phosphate buffer (pH 7.5) for 360 min by a linear gradient, and 0.15 M NaCl in 0.01 M sodium phosphate buffer (pH 7.5) for 120 min. The effluent was monitored by UV absorption at 280 nm and the phenol−sulfuric acid method (*14*) at 490 nm. Desalting the effluent by dialysis against deionized water and freeze-drying gave a purified polysaccharide (1.20 g).

Specific Rotation Measurement. Measurements of optical rotation at 589 nm at 20 °C were made using a DIP-360 (Japan Spectroscopic Co., Ltd., Tokyo, Japan) equipped with a cell with a 10 cm optical path length. The test material was dissolved in distilled water.

Determination of Molecular Weight. The weight-average molecular weight (M_w) of the purified polysaccharide was determined by high-performance size exclusion chromatography coupled with a multiangle laser light scattering (SEC-MALLS) photometer (DAWN-E, Wyatt Technology Corp.). The prepared sample (1.0 mg/mL in water) was injected into an OH-pak SB-806MHQ column (300 × 8 mm i.d., Shoko Co., Ltd., Tokyo, Japan) and eluted with water at a flow rate of 0.5 mL/min. The value of $\delta n/\delta c$ was assumed to be 0.152.

Neutral Sugars Composition by GC Analysis. The purified polysaccharide was partially hydrolyzed with 90% (v/v) formic acid at 100 °C for 6 h, and the formic acid was removed by evaporation in vacuo. Moreover, the hydrolysate was completely hydrolyzed with 2 M trifluoroacetic acid (TFA) at 100 °C for 6 h. After removal of TFA by evaporation in vacuo, the resulting sugars were reduced with sodium borohydride ($NaBH_4$) and then were converted into alditol acetate derivatives with acetic anhydride in an equal volume of pyridine at 120 °C for 2 h (*15*). After removal of solvent by evaporation in vacuo, the sample was dissolved in chloroform and analyzed under the following conditions: instrument, GC-17A (Shimadzu Co., Kyoto, Japan); detector, flame ionization detection (FID); column, DB-225 J&W GC column (30 m × 0.15 μm × 0.25 μm i.d., Agilent Technologies Japan Ltd., Tokyo, Japan); temperatures, injection port at 170 °C and detector at 230 °C; column oven, linear gradient from 170 to 210 °C for 20 min (at 2 °C/min). Peaks were identified by comparing their retention times to that of the standard alditol acetates derived from α-L-rhamnose (α-L-Rha), α-L-arabinose (α-L-Ara), β-D-galactose (β-D-Gal), and D-glucose (β-D-Glc).

Sugar Identification by High-Performance Anion-Exchange Chromatography Equipped with Pulsed Amperometric Detector (HPAEC-PAD) Analysis. The adsorption of WSSP-AGP during anion-exchange column chromatography strongly indicates the presence of some uronic acids. We performed HPAEC-PAD analysis to identify sugars according to the following procedures. The purified polysaccharide was partially hydrolyzed with 90% (v/v) formic acid at 100 °C for 6 h, and the formic acid was removed by evaporation in vacuo. Then, the hydrolysate was completely hydrolyzed with 2 M TFA at 100 °C for 6 h. After removal of TFA by evaporation in vacuo, the sample was injected into a CarboPak PA-1 column (250 × 4 mm i.d., Dionex Inc., Osaka, Japan) and eluted at a flow rate of 1.0 mL/min with 0.20 M NaOH for 5 min followed by a linear gradient from 0 to 0.45 M NaOAc in 0.20 M NaOH for 30 min. The effluent was monitored with the PAD Dionex DXc-500 system, and peaks were identified by comparing their retention times to those of the standard sugars: α-L-Rha, α-L-Ara, β-D-Gal, and β-D-glucuronic acid (β-D-GlcA).

Amino Acid Analysis. Amino acid analysis was performed at TORAY Research Center, Inc. A sample was hydrolyzed at 110 °C for 22 h with 6 M HCl and analyzed by an L-8800 amino acid analyzer (Hitachi High-Technologies Co., Tokyo, Japan). Each peak was identified by comparing its retention time to those of the standard amino acids.

Methylation Analysis. After double methylation according to the method of Ciucanu and Kerek (*16*) and hydrolysis, following the same procedures as described for the analysis of sugars composition, the permethylated polysaccharide was converted to partially methylated alditol acetates by an additional treatment with acetic anhydride in an equal volume of pyridine at 120 °C for 2 h (*15*). These derivatives were analyzed and quantified by GC-MS (GCMS-QP5000, Shimadzu Co.) and used to analyze component sugars under the following conditions: column, DB-225 J&W GC (30 m × 0.15 μm × 0.25 μm i.d., Agilent Technologies Japan Ltd.); column oven, 170 °C for 5 min followed by a linear gradient from 170 to 210 °C for 20 min (at 2 °C/min); syringe needle temperature, 170 °C; and detector temperature, 230 °C. Identification of linkages was made by comparison to the mass spectra of known standards (*17*).

Partial Acidic Hydrolysis and Separation of the Hydrolysate. WSSP-AGP (ca. 100 mg) was partly hydrolyzed with 0.01, 0.05, and 0.10 M TFA (ca. 50 mL) at 100 °C for 1 h. After neutralization with NaOH solution, each hydrolysate was fractionated by injection into a size exclusion column chromatograph using Toyopearl HW-65S (860 × 40 mm i.d.; Tosoh Co.) and eluted at a flow rate of 1.0 mL/min with distilled water. Fractions (17 mL/tube) were collected, and the effluent was monitored by UV absorption at 280 nm and the phenol−sulfuric acid method (*14*) at 490 nm. After freeze-drying, we obtained partially degraded polysaccharide and low molecular weight compounds. The high molecular weight (HMW) fractions obtained from the hydrolysates with 0.01, 0.05, and 0.10 M TFA were 67.0, 36.8, and 26.6 mg, respectively. The latter compounds, separated from the WSSP-AGP hydrolyzed with 0.01 and 0.05 M TFA, were fractionated by HPLC (Shimadzu Co.) by injection into an ODS column chromatograph (DaisoPak SP-120-5-ODS-BP, 250 × 20 mm i.d.; Daiso Co. Ltd., Osaka, Japan) and eluted at a flow rate of 5.0 mL/min with distilled water. Each fraction containing oligosaccharides was collected and the effluent monitored with a refractive index detector.

Mass Spectrometry (MS) Analysis of Low Molecular Weight Fractions from the Hydrolysates of WSSP-AGP. MS analysis of the low molecular weight (LMW) fractions from the WSSP-AGP hydrolyzed with TFA was performed using a Varian 1200/1200 L system equipped with a Varian 1200 L MS/MS (Varian Technologies Japan Ltd., Tokyo, Japan) by the flow injection method (flow rate at 20 μL/min). The operating conditions were as follows: ion mode, positive electrospray ionization (ESI^+); needle voltage, 3.5 kV; shield voltage, 250 V; cone voltage, 45 V; nebulizing gas, nitrogen (52 psi); drying gas, nitrogen (250 °C, 20 psi); and mass range, m/z 100−1500. Hydrolysate samples with 0.01 and 0.05 M TFA were dissolved in 20% MeOH and in 20% MeOH containing 0.25% (v/v) formic acid, respectively, and were analyzed.

NMR Spectroscopy. ^1H and ^{13}C NMR spectra were recorded on JEOL 400 MHz (JNM-AL400) and 600 MHz spectrometers (JNM-ECA600). Each sample (including WSSP-AGP, the HMW fractions from the hydrolysates with 0.01 and 0.10 M TFA) was dissolved in D_2O (2.3−4.0 w/v %) and examined at 80 °C in a 5 mm o.d. tube. Chemical shifts were measured in reference to internal DMSO (δ_H 2.49, δ_C 39.5 relative to TMS). The resolution-enhanced ^1H NMR spectrum was recorded with a spectral width of 11000 Hz in 16000 complex data points. H-decoupled 99.45 MHz ^{13}C NMR spectra were recorded; 32000 complex data points were collected. Prior to FT, noise was reduced using exponential multiplication. DEPT spectra were recorded in 4000 complex data points. $^1H-^1H$ COSY spectra were recorded with a total of 512 spectra of 512 data points with 112 scans/t_1 increment and 1700 Hz width in each dimension. HMQC spectra were recorded with a ^1H frequency of 395.75 MHz (99.5 MHz for ^{13}C), 1400 Hz width for t_2 and 18000 Hz width for t_1. A total of 256 spectra of 256 data points with 720 scans/t_1 increment were recorded. The HMBC spectra were recorded at a ^1H frequency of 600 MHz (150 MHz for ^{13}C) with spectral widths of 5400 Hz for t_2 and 38000 Hz for t_1. A total of 256 spectra of 2000 data points with 32 scans per t_1 increment were recorded.

Animals. Twenty-four male KKA^y mice (5 weeks old) were purchased from CLEA Japan Inc. The mice were housed in an air-conditioned room controlled at 24 ± 2 °C and a relative humidity of 50 ± 10% with a 12 h light/dark cycle. They were fed on standard chow (CE-2, CLEA Japan Inc., Tokyo, Japan) and tap water ad libitum throughout the experiment. This study was carried out in accordance with Guideline for Animal Experimentation No. 88, established by the Prime Minister's Office of Japan in 2006.

Effect of Continuous Ingestion of WSSP-AGP in KKA^y Mice. The mice were randomly divided into three groups of eight animals on the basis of FPG levels after a week of acclimatization. Each group was orally given WSSP-cortex at a dose of 200 mg/kg and WSSP-AGP at a dose of 40 mg/kg daily for 6 weeks, whereas the control group was given only water. Each test sample was freeze-dried and powdered before the

Table 1. Amino Acid Composition of WSSP-AGP

amino acid	composition (mol %)	amino acid	composition (mol %)
aspartic acid	5.6	leucine	2.8
threonine	8.4	tyrosine	0.6
serine	13.7	phenylalanine	1.1
glutamic acid	5.1	lysine	2.8
glycine	5.1	histidine	0.9
alanine	18.2	arginine	0.6
valine	5.0	hydroxyproline	24.5
methionine	0.6	proline	2.8
isoleucine	2.2		
		total	100.0

Table 2. Methylation Analysis of WSSP-AGP

methylated sugar	linkage type	molar ratio	major mass fragments (*m/z*)
2,3,5-Me_3-Ara	Ara-(1→	22.4	87, 101,117, 129, 161
2,3-Me_2-Ara	→5)-Ara-(1→	8.6	87, 101, 117, 129, 189
2-Me-Ara	→3, 5)-Ara-(1→	1.0	85, 99, 117, 127, 159
2,3,4,6-Me_4-Gal	Gal-(1→	1.0	87, 101, 117, 129, 145, 161, 205
2,4,6-Me_3-Gal	→3)-Gal-(1→	5.3	87, 101, 117, 129, 161, 233
2,3,4-Me_3-Gal	→6)-Gal-(1→	2.6	87, 101, 117, 129, 161, 189, 233
2,4-Me_2-Gal	→3, 6)-Gal-(1→	16.2	87, 101, 117, 129, 189, 233

experiment and dissolved in water. Blood samples were collected from the tail vein of each animal every week, and plasma samples were obtained by centrifugation. FPG was measured using plasma samples and a Glucose CII-test Wako (Wako Pure Chemical Industries, Ltd.).

Statistical Analysis. All data were expressed as mean ± SD. Statistical analysis was performed with Turkey−Kramer's multiple-comparison test using Excel add-in software Statcel2 to determine significant differences. $P < 0.05$ was considered to be significant.

RESULTS AND DISCUSSION

A WSSP-AGP from the tuberous cortex of *I. batatas* L. was isolated by the following procedures: (1) extraction of the dried cortex of WSSP with water at room temperature, (2) precipitation by adding solid ammonium sulfate for removal of proteins, (3) separation using hydrophobic interaction column chromatography (Toyopearl Butyl-650M) to obtain a crude polysaccharide fraction, and (4) purification by anion-exchange column chromatography (Toyopearl SuperQ-650M). The purified polysaccharide had a negative specific rotation $[\alpha]_D^{20}$ −37.1 (*c* 0.21, water). Its M_w was 126800 g/mol (estimated using SEC-MALLS). GC and HPAEC-PAD analyses identified its sugar components as α-L-Rha, α-L-Ara, β-D-Gal, and β-D-GlcA in a molar ratio of 1.0:4.1:7.6:1.3. This constituent contained 5% (w/w) protein composed of 17 kinds of amino acids. The major components were hydroxyproline (Hyp) 24.5 mol %, alanine (Ala) 18.2 mol %, and serine (Ser) 13.7 mol % (**Table 1**). This strongly indicates that this compound is a kind of arabinogalactan-protein (AGP).

The result of methylation analysis for WSSP-AGP is shown in **Table 2**. 2,3,5-Tri- and 2,3-di-*O*-methyl-L-arabinose made up most of the detected α-L-Ara*f* residues and were identified as follows: α-L-Ara*f*-(1→ (39.2 mol %) and →5)-α-L-Ara*f*-(1→ (15.1 mol %), respectively. A smaller amount of 2-*O*-methyl-L-arabinose was also detected and identified as →3, 5)-α-L-Ara*f*-(1→ (1.7 mol %). With regard to the β-D-Gal*p* residues, 2,3,4,6-tetra-, 2,4,6-tri-, 2,3,4-tri-, and 2,4-di-*O*-methyl D-galactose were detected and identified as β-D-Gal*p*-(1→ (1.7 mol %), →3)-β-D-Gal*p*-(1→ (9.3 mol %), →6)-β-D-Gal*p*-(1→ (4.6 mol %), and →3, 6)-β-D-Gal*p*-(1→ (28.4 mol %), respectively. A backbone could be (1→3)-β-D-galactan, because the content of 3-linked β-D-Gal*p* residues was higher than that of 6-linked β-D-Gal*p* residues.

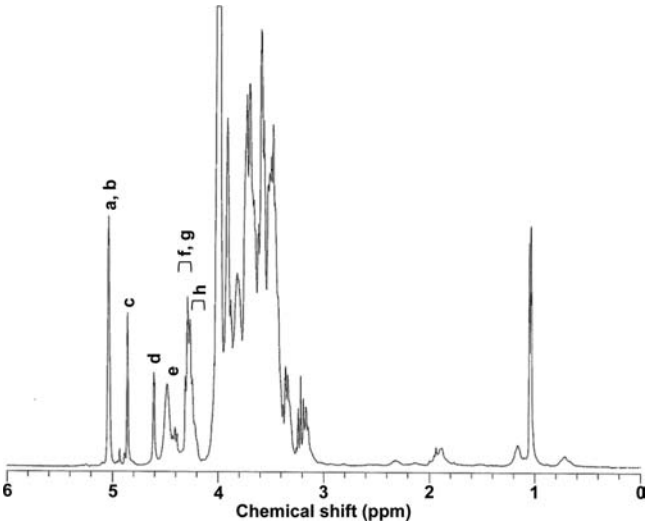

Figure 1. ^{1}H NMR spectrum of WSSP-AGP recorded on a 400 MHz spectrometer in D_2O at 80 °C.

No derivatives from α-L-Rha*p* residue were observed. The methylation analysis in this paper could not give information on the linkage of D-GlcA*p* residue.

To investigate the structure further, we carried out 1D and 2D NMR experiments. **Figure 1** shows a ^{1}H NMR spectrum of WSSP-AGP. The anomeric region (δ_H 4.2−5.1) in the spectrum contains some sharp and overlapping signals, which were assigned by a ^{1}H−^{1}H COSY experiment. Those of sugar residues were arbitrarily labeled **a**−**h** as shown in **Figure 1**. On the basis of their observed chemical shifts, δ_H 5.04 was assigned to **a** and **b**, δ_H 4.86 to **c**, δ_H δ 4.61 to **d**, δ_H 4.39−4.48 to **e**, δ_H 4.27−4.31 to **f**, δ_H 4.28 to **g**, and δ_H 4.24−4.25 to **h**. The ^{13}C NMR spectrum also showed signals in the anomeric region (δ_C 100−111), and δ_C 109.4 was assigned to **a** and **b**, δ_C 108.0 to **c**, δ_C 101.1 to **d**, δ_C 103.8−104.2 to **e** and **f**, δ_C 103.1 to **g**, and δ_C 103.6 to **h** (**Figure 2**). The DEPT experiment revealed that δ_C 61.6 was assigned to methylene signals of the C-5 of **a** and **c**, and δ_C 62.0 was assigned to C-6 of β-D-Gal*p*-(1→ and →3)-β-D-Gal*p*-(1→. In addition, two methylene signals of C-5 of **b**, →5)-α-L-Ara*f*-(1→, and C-6 of **f** and **h**, →3, 6)-β-D-Gal*p*-(1→ and →6)-β-D-Gal*p*-(1→, appeared as negative peaks at δ_C 67.5, 69.1−69.3, and 69.4−69.7, respectively. These assignments were consistent with the downfield shift associated with substitution at the C-5 and C-6 positions. Cross-peaks in the HMQC spectrum revealed that δ_C 79.8 was assigned to C-4 of **g**, →4)-β-D-GlcA*p*-(1→, and δ_C 80.6 was assigned to C-3 of **e** and **f**, →3, 6)-β-D-Gal*p*-(1→. This suggests the following residues: **a**, α-L-Ara*f*-(1→; **b**, →5)-α-L-Ara*f*-(1→; **c**, α-L-Ara*f*-(1→ linked at the O-5 position of →5)-α-L-Ara*f*-(1→; **d**, α-L-Rha*p*-(1→; **f**, →3, 6)-β-D-Gal*p*-(1→; **g**, →4)-β-D-GlcA*p*-(1→; and **h**, →6)-β-D-Gal*p*-(1→ (**Table 3**). In the HMBC spectrum of WSSP-AGP, several cross-peaks were observed (**Figure 3**). Five of them could be assigned to glycosidic linkages [(**a** H-1, **f** C-3) to **a1→f3**, (**c** H-1, **b** C-5) to **c1→b5**, (**d** H-1, **g** C-4) to **d1→g4**, (**g** H-1, **h** C-6) to **g1→h6**, and (**f** H-1, **f** C-6) to **f1→f6**]. The correlation of **a1→f3** suggested that α-L-Ara*f*-(1→ and →5)-α-L-Ara*f*-(1→ were attached to C-3 (δ_C 80.6) of →3, 6)-β-D-Gal*p*-(1→, in accordance with the previous assignment of branched structure of β-D-galactan attached with α-L-Ara*f* (*18*−*21*). The cross-peak **c1→b5** indicates the existence of an α-L-Ara*f*-(1→5)-α-L-Ara*f*-(1→. Although **a** and **c** were assigned to α-L-Ara*f*-(1→ residues, **a** is attached to the O-3 position of →3, 6)-β-D-Gal*p*-(1→, whereas **c** is attached to the O-5 position of →5)-α-L-Ara*f*-(1→. A cross-peak of **d1→g4** suggested the existence of α-L-Rha*p*-(1→4)-β-D-GlcA*p*-(1→, although the α-L-Rha*p* residue was not detected in methylation

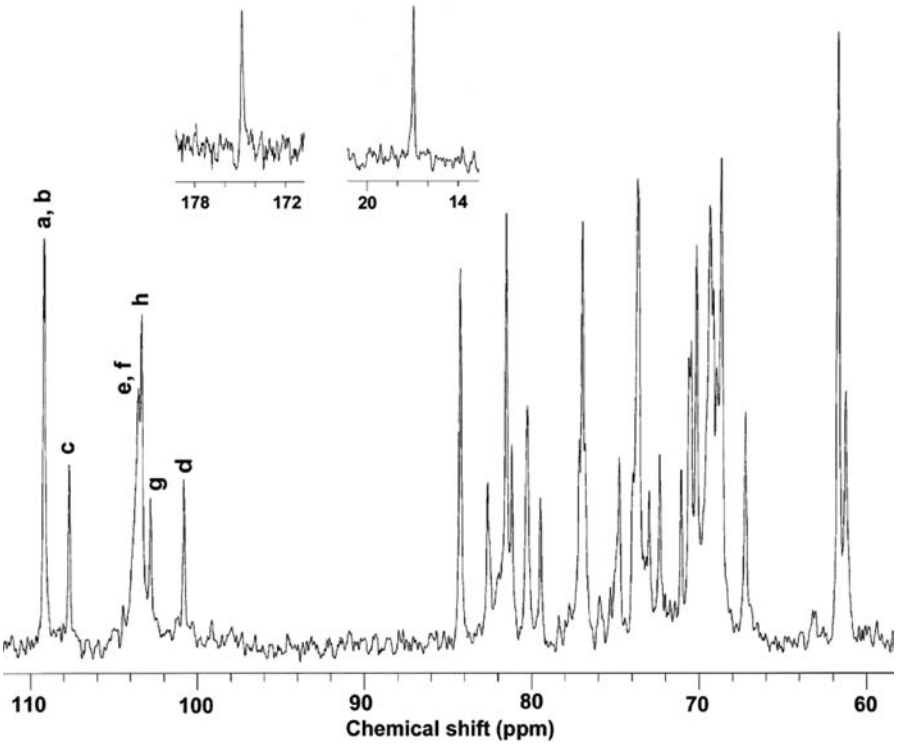

Figure 2. ^{13}C NMR spectrum of WSSP-AGP recorded on a 400 MHz spectrometer in D_2O at 80 °C.

Table 3. Assignment of ^{1}H and ^{13}C NMR Spectra of WSSP-AGP

		chemical shift (ppm)					
residue		1	2	3	4	5	6
a, Ara-(1→[a]	^{1}H	5.04	3.97	3.74	3.92	3.50, 3.59	
	^{13}C	109.4	81.8	77.2	84.6	61.6	
b, →5)-Ara-(1→	^{1}H	5.04	3.97	3.81	4.00	3.60, 3.68	
	^{13}C	109.4	81.8	77.3	81.8	67.5	
c, Ara-(1→[a]	^{1}H	4.86	3.92	3.74	4.00	3.50, 3.59	
	^{13}C	108.0	81.5	77.2	81.8	61.6	
d, Rha-(1→	^{1}H	4.61	3.72	3.55	3.22	3.79	1.05
	^{13}C	101.1	70.9	70.8	72.7	69.0	17.2
e, →3,6)-Gal-(1→[b]	^{1}H	4.39−4.48	NA[c]	3.55−3.59	NA	NA	NA
	^{13}C	103.8−104.2	NA	80.6	NA	NA	NA
f, →3,6)-Gal-(1→[b]	^{1}H	4.27−4.31	3.43	3.55−3.59	3.93	3.74	3.89−4.06
	^{13}C	103.8−104.2	70.4	80.6	69.0	73.9	69.1−69.3
g, →4)-GlcA-(1→	^{1}H	4.28	3.17	3.37	3.42	3.55	
	^{13}C	103.1	74.0	75.1	79.8	70.9	174.9
h, →6)-Gal-(1→	^{1}H	4.24−4.25	3.34	3.48	3.92	3.75	3.79−3.86
	^{13}C	103.6	71.4	73.3	69.0	73.9	69.4−69.7

[a] Residue **a** was a terminal arabinosyl residue attached to the O-3 position of the galactosyl residues, whereas residue **c** was a terminal arabinosyl residue attached to the O-5 position of the arabinosyl residue of **b**. [b] Residues **e** and **f** were assigned to a backbone core, (1→3)-β-D-galactan, and side chain, (1→6)-β-D-galactan, respectively. [c] Not assigned.

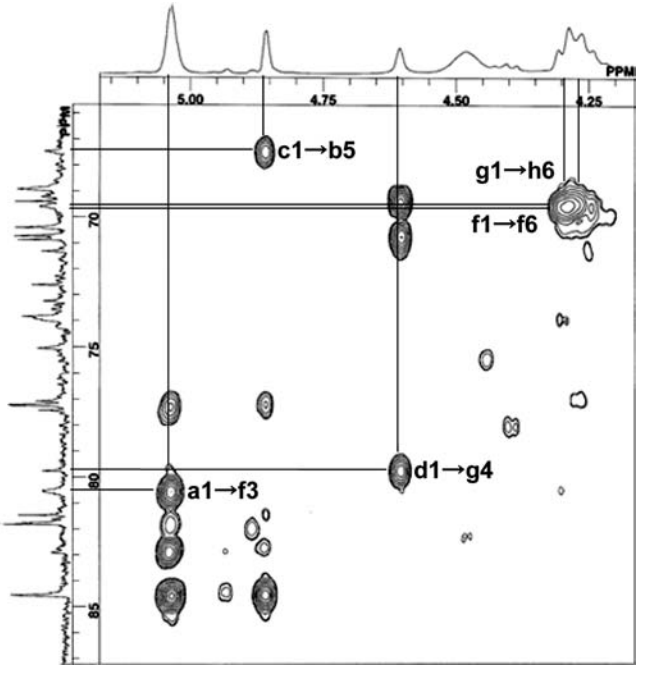

Figure 3. HMBC spectrum of WSSP-AGP recorded on a 600 MHz spectrometer in D_2O at 80 °C.

analysis. The correlation between H-1 (δ_H 4.61) of the α-L-Rha*p* residue and C-4 (δ_C 79.8) of →4)-β-D-GlcA*p*-(1→ was not observed for the HMW fraction from the hydrolysate. This suggests that the **d**, α-L-Rha*p*, residue is present only as a terminating group. The correlation between **f**, →3, 6)-β-D-Gal*p*-(1→ (δ_H 4.27−4.31), and C-6 (δ_C 69.1−69.3) of the β-D-Gal*p* residues indicates as follows: C-3 positions of **f** were attached not to β-D-Gal*p* residues but to α-L-Ara*f* residues. Residue **g**, →4)-β-D-GlcA*p*-(1→ (δ_H 4.28), only correlated with the C-6 (δ_C 69.4−69.7) of **h**, →6)-β-D-Gal*p*-(1→, and the C-6 of (1→6)-β-D-galactan was attached to α-L-Rha*p*-(1→4)-β-D-GlcA*p*-(1→ as a terminal residue.

On the other hand, only one cross-peak was observed between proton **e** (δ_H 4.39−4.48) and anomeric carbons (δ_H 103.8−104.2) in the HMQC spectrum and the $^{1}H-^{1}H$ COSY and HMBC spectra showed no correlation with **e** or the others. As shown in

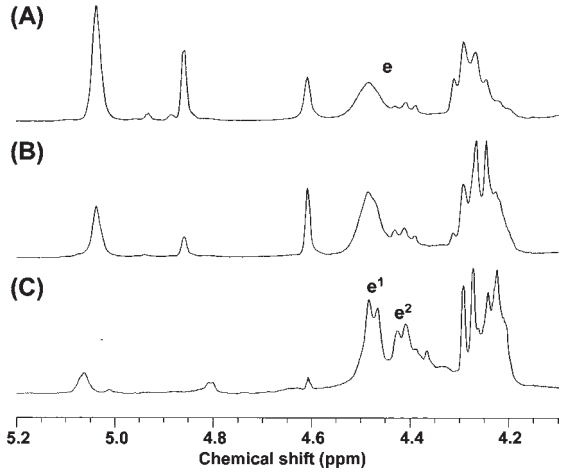

Figure 4. ^{1}H NMR spectra of WSSP-AGP and high molecular weight fractions from the hydrolysates recorded on a 400 MHz spectrometer in D_2O at 80 °C. Spectra represent the WSSP-AGP (**A**) and HMW fractions from the WSSP-AGP hydrolyzed with 0.01 M TFA (**B**) or with 0.10 M TFA (**C**).

Figure 1, the signal had a very broad shape, which was presumably caused by increased steric hindrance due to high branching. The WSSP-AGP was partly degraded by acid hydrolysis and broken into low molecular weight components, which were analyzed by 1D and 2D NMR spectra. The ^{1}H NMR spectra of the HMW fractions from 0.01 and 0.10 M TFA hydrolysates are shown in panels **B** and **C**, respectively, of **Figure 4**. These show a significant decrease in anomeric protons (δ_H 4.61−5.04) corresponding to α-L-Ara*f* and α-L-Rha*p* residues associated with the rise in TFA concentration when compared with that of WSSP-AGP. This result suggests that outside chains composed of α-L-Ara*f* and α-L-Rha*p* residues may be selectively hydrolyzed and removed from the polysaccharide chain of WSSP-AGP. In **Figure 4C**, the signals at 4.47 ppm and 4.41 ppm were labeled $\mathbf{e^1}$ and $\mathbf{e^2}$, respectively. The ^{1}H−^{1}H COSY spectra suggest that $\mathbf{e^1}$ and $\mathbf{e^2}$ were derived from (1→3)-β-D-galactan composed of →3, 6)-β-D-Gal*p*-(1→ and →3)-β-D-Gal*p*-(1→. In addition, the HMBC spectrum of the HMW fraction from 0.10 M TFA hydrolysate clearly showed a cross-peak between $\mathbf{e^1}$ and C-3 (δ_C 80.6) of the β-D-galactan. The same correlation was detected for $\mathbf{e^2}$, although it was weak. The findings in this experiment suggest that $\mathbf{e^1}$ and $\mathbf{e^2}$ (corresponding to **e**) can be attributed to the (1→3)-β-D-galactan backbone.

The HPAEC-PAD chromatograms of the LMW fractions from 0.01, 0.05, and 0.10 M TFA hydrolysates are shown in spectra **A**, **B**, and **C**, respectively, of **Figure 5**. A peak was detected at 13.70 min in the 0.01 M TFA hydrolysate chromatogram (**Figure 5A**), but not in the other two (**Figure 5B**,**C**). MS analysis suggested that this peak corresponds to an arabinobiose, because the MS spectrum contained a peak at *m*/*z* 305.3 attributed to $[Ara_2 + Na]^+$. Many peaks detected at 5−15 min were similar to those in the spectra reported by Yamada et al. (*22*). These peaks were assigned to a series of 6-linked galactosyl oligosaccharides by MALDI-TOF-MS analysis. Therefore, their peaks shown in **Figure 5B** and **5C** may correspond to 6-linked β-D-Gal*p* residues. With regard to the several peaks detected at 17−18 min (**Figure 5B**,**C**), MS analysis of this fraction showed that *m*/*z* 365.1, 527.2, 689.3, and 851.4 could correspond to $[Rha - GlcA + Na + 2H]^+$, $[Rha - GlcA - Gal + Na + 2H]^+$, $[Rha - GlcA - Gal_2 + Na + 2H]^+$, and $[Rha - GlcA - Gal_3 + Na + 2H]^+$, respectively. This suggests that β-D-GlcA*p* residues formed oligomers with α-L-Rha*p* residues and also supports the identification of partial structures of side chains.

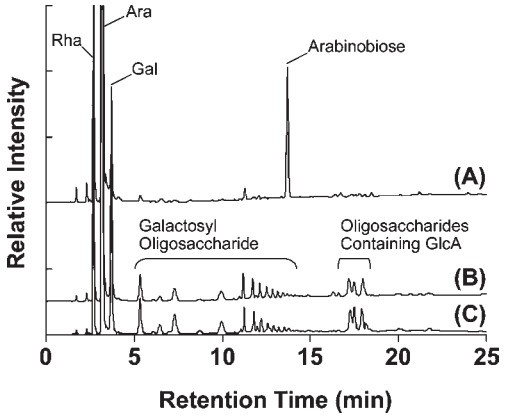

Figure 5. HPAEC-PAD chromatograms of the low molecular weight fractions from the hydrolysates of WSSP-AGP. Each chromatogram represents the LMW fraction of the WSSP-AGP hydrolyzed with 0.01 M TFA (**A**), 0.05 M TFA (**B**), or 0.10 M TFA (**C**), respectively.

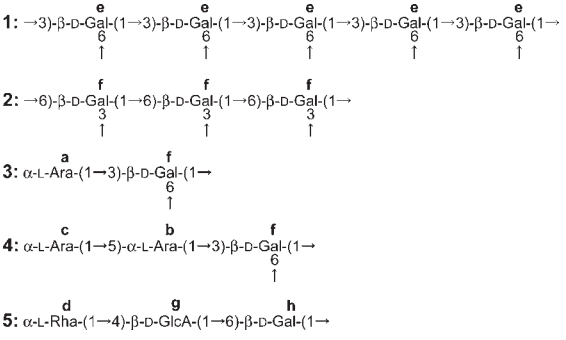

Figure 6. Partial structures of WSSP-AGP.

On the basis of the above, five possible partial structures are shown in **Figure 6**. WSSP-AGP has the following structural features: a partial structure **1**, a (1→3)-β-D-galactan backbone highly substituted at O-6 with additional β-galactosyl units such as partial structure **2**, (1→6)-β-D-galactan containing partial structures **3**−**5**. The structure of WSSP-AGP is similar to those of *Acacia senegal* (*20*), *Nicotiana* spp. (*19*, *21*), and the coffee bean (*23*).

AGPs are well-known as potential immunological modulators (*22*, *24*), although there is little direct evidence for their antidiabetic influence. The hypoglycemic effects in alloxan-induced diabetic rabbits of AGPs from green tea (*25*) and the fruit of *Lycium barbarum* (*26*, *27*) have already been studied. However, their structural characterization such as composition of sugars and linkage of each sugar residue is not known in detail. AGP isolated from *Acacia senegal*, the structure of which is understood in detail (*28*), has no hypoglycemic effect in diabetic model animals (*29*). The hypoglycemic effect of AGP is not completely understood. Thus, we orally administered WSSP-AGP to KKA^y mice for 6 weeks. As shown in **Figure 7**, FPG after 4 weeks in the WSSP-AGP group (4 weeks, 302.7 ± 77.7 mg/dL*; 5 weeks, 311.6 ± 63.9 mg/dL*; and 6 weeks, 305.4 ± 76.9 mg/dL*) was significantly lower than that of the control group (4 weeks, 392.4 ± 77.3 mg/dL; 5 weeks, 405.2 ± 103.0 mg/dL; and 6 weeks, 395.8 ± 86.7 mg/dL). This suggests that WSSP-AGP has a crucial role in the hypoglycemic effect of WSSP.

In recent years, it has been theorized that changes in gut microflora and inflammation are closely related to the appearance and development of obesity and diabetes (*30*−*33*). We found that WSSP-AGP is selectively fermented by one of the beneficial

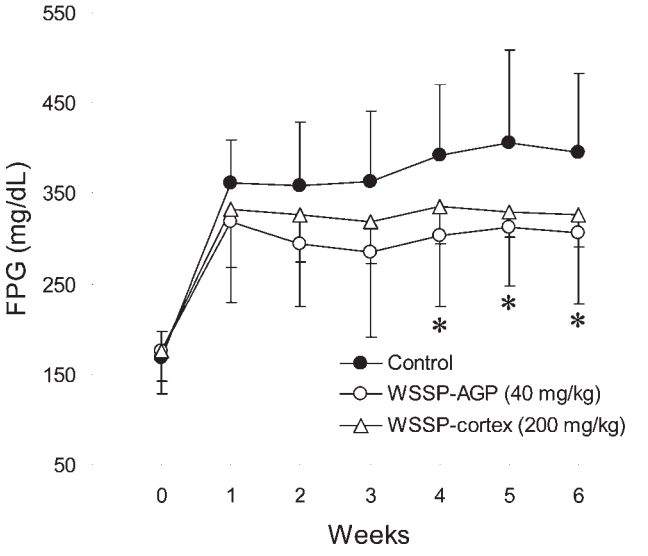

Figure 7. Effect of WSSP-AGP on fasting plasma glucose levels in KKA^y mice. Animals were randomly divided as follows: untreated (control), treated with WSSP-AGP, and treated with WSSP-cortex. The doses of WSSP-AGP and WSSP-cortex were 40 and 200 mg/kg/day, respectively. The test materials were suspended in water. The control group was given only water. All values represent the mean ± SD (n = 6). P values were calculated by Tukey−Kramer's test. Significant differences in glucose level versus that of the control group: *, $P < 0.05$.

bacteria, *Bifidobacterium longum*, isolated from human microflora. We also found that WSSP-AGP showed intestinal immunological activity through Peyer's patch, but how these biological facts can be related to antidiabetic effects is a subject for further study.

In conclusion, we characterized an arabinogalactan-protein that we isolated from WSSP. It is clear that this polysaccharide shows the hypoglycemic effects of WSSP, although the mechanism is not yet understood in detail. These studies are currently in progress.

ACKNOWLEDGMENT

We thank Dr. T. Sakamoto, Associate Professor at Osaka Prefecture University, for HPAEC-PAD analysis.

LITERATURE CITED

(1) Noda, N.; Yoda, S.; Kawasaki, T.; Miyahara, K. Resin glycosides. XV. Simonins I−V, ether-soluble resin glycoside (Jalapins) from the roots of *Ipomoea batatas* (cv. Simon). *Chem. Pharm. Bull.* **1992**, *40*, 3163−3168.

(2) Yang, T. "Shirokansyo Simon", personal publication, Kochi, Japan, 1974, Vol.1; and 1975, Vol. 2.

(3) Kusano, S.; Abe, H.; Okada, A. Study of antidiabetic activity of white skinned sweet potato (*Ipomoea batatas* L.): comparison of normal and streptozotocin induced diabetic rats and hereditary diabetic mice. *Nippon Nogeikagaku Kaishi* **1998**, *72*, 1045−1052.

(4) Kusano, S.; Abe, H. Antidiabetic activity of white skinned sweet potato (*Ipomoea batatas* L.) in obese zucker fatty rats. *Biol. Pharm. Bull.* **2000**, *23*, 23−26.

(5) Kusano, S.; Tamasu, S.; Nakatsugawa, S. Effects of the white skinned sweet potato (*Ipomoea batatas* L.) on the expression of adipocytokine in adipose tissue of genetic type 2 diabetic mice. *Food Sci. Technol. Res.* **2005**, *11*, 369−372.

(6) Ludvik, B.; Waldhäusl, W.; Prager, R.; Kautzky-Willer, A.; Paccini, G. Mode of action of *Ipomoea batatas* (caiapo) in type 2 diabetic patients. *Metabolism* **2003**, *52*, 875−880.

(7) Ludvik, B.; Neuffer, B.; Paccini, G. Efficacy of *Ipomoea batatas* (caiapo) on diabetes control in type 2 diabetic subjects treated with diet. *Diabetes Care* **2004**, *27*, 436−440.

(8) Ludvik, B.; Hanefeld, M.; Paccini, G. Improved metabolic control by *Ipomoea batatas* (caiapo) is associated with increased adiponectin and decreased fibrinogen levels in type 2 diabetic subjects. *Diabetes Obes. Metab.* **2008**, *10*, 586−592.

(9) Oke, J. M.; Oladosu, B.; Okunola, M. C. Sweet potato (*Ipomoea batatas*) tuber-potential oral anti-diabetic agent. *Afr. J. Biomed. Res.* **1999**, *2*, 13−17.

(10) Kusano, S.; Abe, H.; Tamura, H. Isolation of antidiabetic components from white-skinned sweet potato (*Ipomoea batatas* L.). *Biosci., Biotechnol., Biochem.* **2001**, *65*, 109−114.

(11) Kelly, G. S. Larch arabinogalactan: clinical relevance of a novel immune-enhancing polysaccharide. *Altern. Med. Rev.* **1999**, *4*, 96−103.

(12) Edwards, S.; Chaplin, M. F.; Blackwood, A. D.; Dettmar, P. W. Primary structure of arabinoxylans of ispaghula husk and wheat bran. *Proc. Nutr. Soc.* **2003**, *62*, 217−222.

(13) Sood, N.; Baker, W. L.; Coleman, C. I. Effect of glucomannan on plasma lipid and glucose concentrations, body weight, and blood pressure: systematic review and meta-analysis. *Am. J. Clin. Nutr.* **2008**, *88*, 1167−1175.

(14) Dubois, M.; Gilles, S. A.; Hamilton, J. K.; Rebers, P. A.; Smith, F. Colorimetric method for determination of sugars and related substances. *Anal. Chem.* **1956**, *28*, 350−356.

(15) Slonker, J. H. Gas−liquid chromatography of alditol acetates. *Methods Carbohydr. Chem.* **1972**, *6*, 20−24.

(16) Ciucanu, I.; Kerek, F. A simple and rapid method for the permethylation of carbohydrates. *Carbohydr. Res.* **1984**, *131*, 209−217.

(17) Jansson, P. E.; Kenne, L.; Liedgren, H.; Lindberg, B.; Lönngren, J. A practical guide to the methylation analysis of carbohydrates. *Chem. Commun., Univ. Stockholm* **1976**, *8*, 1−75.

(18) Wagner, H.; Jordan, E. An immunologically active arabinogalactan from *Viscum album* 'Berries'. *Phytochemistry* **1988**, *27*, 2511−2517.

(19) Tan, L.; Qiu, F.; Lamport, D. T.; Kieliszewski, M. J. Structure of a hydroxyproline (Hyp)-arabinogalactan polysaccharide from repetitive Ala-Hyp expressed in transgenic *Nicotiana tabacum*. *J. Biol. Chem.* **2004**, *279*, 13156−13165.

(20) Islam, A. M.; Phillips, G. O.; Sljivo, A.; Snowden, M. J.; Williams, P. A. A review of recent developments on the regulatory, structural and functional aspects of gum arabic. *Food Hydrocolloids* **1997**, *11*, 493−505.

(21) Gane, A. M.; Craik, D.; Munro, S. L.; Howlett, G. J.; Clarke, A. E.; Bacic, A. Structural analysis of the carbohydrate moiety of arabinogalactan-proteins from stigmas and styles of *Nicotiana alata*. *Carbohydr. Res.* **1995**, *277*, 67−85.

(22) Taguchi, I.; Kiyohara, H.; Matsumoto, T.; Yamada, H. Structure of oligosaccharide side chains of an intestinal immune system modulating arabiogalactan isolated from rhizomes of *Atractylodes lancea* DC. *Carbohydr. Res.* **2004**, *339*, 763−770.

(23) Nunes, F. M.; Reis, A.; Silva, A. M.; Domingues, M. R.; Coimbra, M. A. Rhamnoarabinosyl and rhamnoarabinoarabinosyl side chains as structural features of coffee arabinogalactans. *Phytochemistry* **2008**, *69*, 1573−1585.

(24) Pettolino, F.; Liao, M. L.; Zhu, Y.; Mau, S. L.; Bacic, A. Structure, function and cloning of arabinogalactan-proteins (AGPs): an overview. *Foods Food Ingredients J. Jpn.* **2006**, *211*, 12−25.

(25) Zhou, X.; Wang, D.; Sun, P.; Bucheli, P.; Li, L.; Hou, Y.; Wang, J. Effects of soluble tea polysaccharides on hyperglycemia in alloxan-diabetic mice. *J. Agric. Food Chem.* **2007**, *55*, 5523−5528.

(26) Luo, Q.; Cai, Y.; Yan, J.; Sun, M.; Corke, H. Hypoglycemic and hypolipidemic effects and antioxidant activity of fruits extracts from *Lycium barbarum*. *Life Sci.* **2004**, *76*, 137−149.

(27) Peng, X. M.; Tian, G. Y. Structural characterization of the glycan part of glycoconjugate LbGp2 from *Lycium barbarum* L. *Carbohydr. Res.* **2001**, *331*, 95−99.

(28) Sanchez, C.; Schmidtt, C.; Kolodziejczyk, E.; Lapp, A.; Gaillard, C.; Renard, D. The acacia gum arabinogalactan fraction is athin oblate ellipsoid: a new model based on small-angle neutron scattering and Ab initio calculation. *Biophys. J.* **2008**, *94*, 629−639.

(29) Ali, B. H.; Ziada, A.; Blunden, G. Biological effects of gum arabic: a review of some recent research. *Food Chem. Toxicol*. **2009**, *47*, 1−8.
(30) Creely, S. J.; McTernan, P. G.; Kusminski, C. M.; Fischer, M.; Da Silva, N. F.; Khanolkar, M.; Evans, M.; Harte, A. L.; Kumar, S. Lipopolysaccharide activates an innate immune system response in human adipose tissue in obesity and type 2 diabetes. *Am. J. Physiol. Endocrinol. Metab*. **2007**, *292*, 740−747.
(31) Cani, P. D.; Amar, J.; Iglesias, M. A.; Poggi, M.; Knauf, C.; Bastelica, D.; Neyrinck, A. M.; Fava, F.; Tuohy, K. M.; Chabo, C.; Waget, A.; Delmée, E.; Cousin, B.; Sulpice, T.; Chamontin, B.; Ferrières, J.; Tanti, J. F.; Gibson, G. R.; Casteilla, L.; Delzenne, N. M.; Alessi, M. C.; Burcelin, R. Metabolic endotoxemia initiates obesity and insulin resistance. *Diabetes* **2007**, *56*, 1761−1772.
(32) Cani, P. D.; Bibiloni, R.; Knauf, C.; Waget, A.; Neyrinck, A. M.; Delzenne, N. M.; Burcelin, R. Changes in gut microbiota control metabolic endotoxemia-induced inflammation in high-fat diet-induced obesity and diabetes in mice. *Diabetes* **2008**, *57*, 1470−1481.
(33) Cani, P. D.; Neyrinck, A. M.; Fava, F.; Knauf, C.; Burcelin, R.; Tuohy, K. M.; Gibson, G. R.; Delzenne, N. M. Selective increases of bifidobacteria in gut microflora improve high-fat-diet-induced diabetes in mice through a mechanism associated with endotoxaemia. *Diabetologia* **2007**, *50*, 2374−2383.

Received for review April 6, 2010. Revised manuscript received September 30, 2010. Accepted October 10, 2010.